Polymer 51 (2010) 535–539

Contents lists available at ScienceDirect

Polymer

journal homepage: www.elsevier.com/locate/polymer

Fibre reinforced nanocomposites: Mechanical properties of PA6/clay and glass fibre/PA6/clay nanocomposites

Mike J. Clifford [a,*], Tong Wan [b]

[a] Faculty of Engineering, The University of Nottingham, University Park, Nottingham NG7 2RD, UK
[b] School of Material Science and Chemical Engineering, Tianjin University of Science and Technology, TEDA, Tianjin 300457, PR China

ARTICLE INFO

Article history:
Received 30 March 2009
Received in revised form
20 July 2009
Accepted 23 November 2009
Available online 27 November 2009

Keywords:
Halpin-Tsai
Nanocomposites
Short fibre

ABSTRACT

In this paper, the effect of two different reinforcements: clay at the nanoscale and glass fibres at the micro-scale, on the mechanical properties of PA/clay and GF/PA/clay are studied. The Halpin-Tsai model is used to predict the modulus of PA/Clay and GF/PA/Clay, both of which are influenced by two factors: reinforcement shape and volume fraction. The relationships between the modulus and reinforcement shape and volume fraction are discussed. Tensile modulus, measured in tensile tests is used to fit the Halpin-Tsai models. The results demonstrate a synergy between the reinforcements at the two different scales.

1. Introduction

Fibre reinforced composites represent an attempt to improve the properties of engineering plastics by the inclusion of stiff, strong fibres. Continuous fibre reinforcements represent the optimum geometric solution, but restrict the processing options available to manufactures [1]. The inclusion of short reinforcing fibres into a plastic matrix generally increases the viscosity of the polymer melt, but enables rapid, high-volume manufacture using injection moulding. Higher fibre volume fractions lead to higher viscosity, so there is a practical limit on fibre volume fraction of around 40%, which limits the application of such materials for structural composite components.

Recently, it has been shown that the inclusion of clay in polyamide 6 leads to an increase in viscosity and also leads to an enhancement in mechanical properties such as Young's modulus [2,3]. It is therefore interesting to consider a polymer with reinforcement on two scales; microscopic fibre reinforcement, combined with exfoliated nanoscale platelets. In this paper we show that there is considerable synergy in this approach. The nanoscale reinforcement contributes to an increase in the tensile modulus of the composites and the prediction is applied by the Halpin-Tsai model.

Polyamide 6/clay (PA/clay) nanocomposites have attracted great industrial interest due to potential applications in producing films, fibres and engineering materials. PA/clay nanocomposites exhibit significant improvements in mechanical and gas barrier properties over conventional composites. These can be attributed to a high exfoliation of clay and strong interaction between clay layers and the PA matrix, which leads to some unique properties [4,5]. X-ray Diffraction (XRD)results show that the crystalline form of PA is changed from α to γ in the presence of clay [6,7]. Fourier Transform infrared spectroscopy (FTIR) results indicate that amide vibrations of PA shift to high wavenumbers in PA/clay nanocomposites, also, Si–O vibrations of clay layers in PA nanocomposites shift with small strain deformation [8,9]. This demonstrates that clay layers are fairly elastic and has a good interface with the PA matrix.

2. Experimental section

The materials used in this study were Ultramid B3 Polyamide 6 (PA): a commercial product supplied by BASF. The Southern Clay Company supplied the clay, Cloisite 30B, as a white powder containing montmorillonite (70%wt) intercalated with an organo modifier (30%wt). E-glass fibres (GF), TufRov 4588 were supplied by PPG. The glass fibres were compatible with PA.

Melt compounding of PA with various clay loadings was achieved in a Rondol 24:1 L/D twin-screw extruder. The processing temperatures for the four zones were set at 230/235/240/245 °C. A high shear rate was applied to break up agglomerates and exfoliate the clay. However, a low shear rate was

* Corresponding author. Tel.: +44 115 8466134; fax: +44 115 9513800.
E-mail address: mike.clifford@nottingham.ac.uk (M.J. Clifford).

0032-3861/$ – see front matter © 2009 Elsevier Ltd. All rights reserved.
doi:10.1016/j.polymer.2009.11.046

crucial to produce GF/PA and GF/PA/Clay composites, to achieve fibre wet out and avoid reducing the mean fibre length too much. GF/PA and GF/PA/Clay were produced in the twin-screw extruder. After some initial trials, the screw speed was set at 50 rpm as this was found to be sufficient to exfoliate the clay without degrading fibre length too much. The diameter of die was 3 mm. Prior to extrusion PA6 and organoclay were dried in a vacuum oven at 80 °C for at least 4 h. The extrudates were pelletized with a Hake pelletizer.

The pellets were injection-moulded into a dog-bone standard mould using an MCP Minimoulder 12/90 HSP injection moulding machine. The process of injection moulding depends on getting the right combination of four variables: the time cycle, the cylinder temperature, the injection pressure and mould temperature. The temperature profiles of the three zones of injection moulding were set at different levels. The cycle time was fixed at 40 s. The injection pressure was fixed at 752 Bar. The temperature of the mould was maintained at 80 °C by circulating water at a constant temperature through channels in the walls of the mould.

Tensile tests were performed on the dog-bone specimens using an Instron-5582 at room temperature according to BS2782-3:326F:1997. The crosshead speed was set at 0.5 mm/min for measuring tensile modulus and at 10 mm/min to measure elongation and ultimate tensile strength. Strain was recorded using an extensometer with a gauge length of 25 mm. Eight specimens were tested for each batch. Young's modulus, tensile strength and elongation to failure were recorded from the stress-strain curves.

3. Modulus prediction using the Halpin-Tsai model

It is well-known that including a modest amount of nanocomposites into a polymer matrix can increase the tensile modulus. This improvement is governed by two factors: the strong interaction between polymers and the clay surface, and the modulus and geometry of the clay reinforcement. A good interface increasing the bond strength, is important for applying modulus prediction models. It is reasonable to assume that a strong interface provides no interfacial sliding in the elastic range. Thus, the reinforcement mechanism in nanocomposites could be similar to that in traditional composites. The modulus of PA/Clay is dependent on the modulus, the volume fraction and the degree of exfoliation of the clay particles. An improvement of the exfoliation increases the aspect ratio and the numbers of particles. These factors are related to the properties of clay layers, which can contribute to the mechanical properties of nanocomposites. A simple and crucial question is whether the significant improvements in mechanical properties can be explained by conventional composites theory. For example, important factors such as aspect ratio, modulus and volume fraction are already well explained and demonstrated in fibre composites, and many composites models take these factors into account. An assumption inherent in all of these theories is that each component of a composite acts independently of the other. The Halpin-Tsai model can be used to predict the stiffness of composites as a function of aspect ratio. Aspect ratio is an important factor in nanocomposites, and is related to the level of the exfoliation. Another objective of this paper is to try to model the modulus of GF/PA/Clay and to evaluate the synergy (if any) in combing the two scales of reinforcement.

The Halpin-Tsai is the most widely used model to predict Young's modulus of composites [10]. It is a simple universal equation, and can be applied to many composites materials. The Halpin-Tsai model described in Equation (1) has been used to compute the modulus of most filler systems and fibre composites [11,12].

$$\frac{E_c}{E_m} = \frac{\left(1+\xi\eta V_f\right)}{1-\eta V_f} \text{ in which } \eta = \frac{E_f/E_m - 1}{E_f/E_m + \xi} \tag{1}$$

where E_c = composite modulus; E_m = matrix modulus; E_f = fibre modulus; V_f = filler or fibre volume fraction; ξ = shape factor, depending on geometry and aspect ratio and orientation [13–16].

It is difficult to calculate the average shapes, sizes and levels of exfoliation, because it involves extensive work that does not provide accurate values, as the particles can have different shapes, sizes and thicknesses. It is important to emphasize that complexities arise when measuring the real aspect ratio of clay, since the images from TEM can show disparity in terms of the length of clay, which depends on the cutting position.

For real materials, when the modulus of the composite, matrix and filler are known, the Halpin-Tsai model can also be used to back-calculate the aspect ratio of the reinforcing particles. This will be an *effective* aspect ratio, which is a reasonable estimate of the average aspect ratio, and provides a useful parameter to compare different nanocomposite compositions. However, the aspect ratio of the clay layers does not need to be measured since we use shape factor ξ to predict the effect on the modulus. In order to understand, comprehensively, the effect of two types of reinforcements, an ideal state is considered. To simplify the analysis, we assume that all clay and fibres are fully aligned, asymmetric and uniform, in both shape and size in the load direction. As we shall see, this assumption generates a model which gives reasonable predictions, but the underlying assumptions will be addressed in future work. The Halpin-Tsai model for PA/Clay (E_m = 1.8 GPa, $E_{f(clay)}$ = 172 GPa) is shown in Fig. 1. The modulus predictions for clay volume range from 1% to 5%, which is within the range for practical nanocomposites. As expected, the Halpin-Tsai equation predicts the effect of calculated shape factor on the relative modulus. Increasing the aspect ratio results in higher reinforcement for a given filler modulus and volume fraction. Clay platelets are hardly effective at both very low ($\xi < 10$) and very high aspect ratios ($\xi > 500$). The modulus significantly increases with high aspect ratio ($20 < \xi < 500$). This means that the modulus is affected by platelet shape and exfoliation. Consequently, when exfoliation is not optimal, the resulting reduction in ξ reduces the modulus. Fig. 2 shows the effect of ξ and $V_{f(glass)}$ on the relative modulus of GF/PA along the longitudinal axis predicted by the Halpin-Tsai equations with E_m = 1.8 GPa, and $E_{f(glass)}$ = 75 GPa. Glass fibres do not have

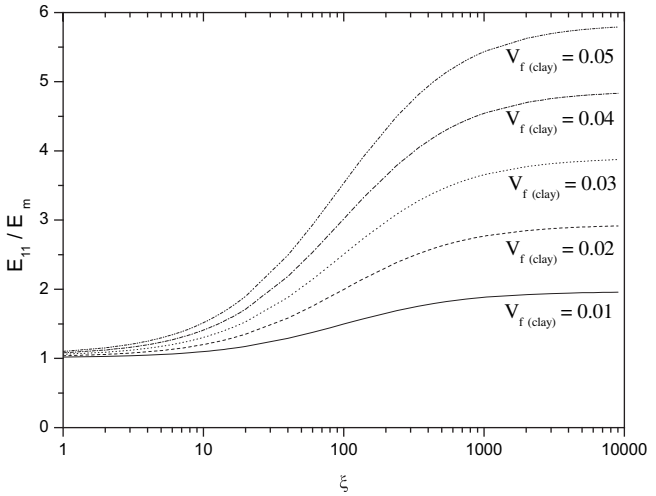

Fig. 1. The effect of ξ and $V_{f(clay)}$ on the relative modulus of PA/Clay along the longitudinal axis predicted by the Halpin-Tsai equations.

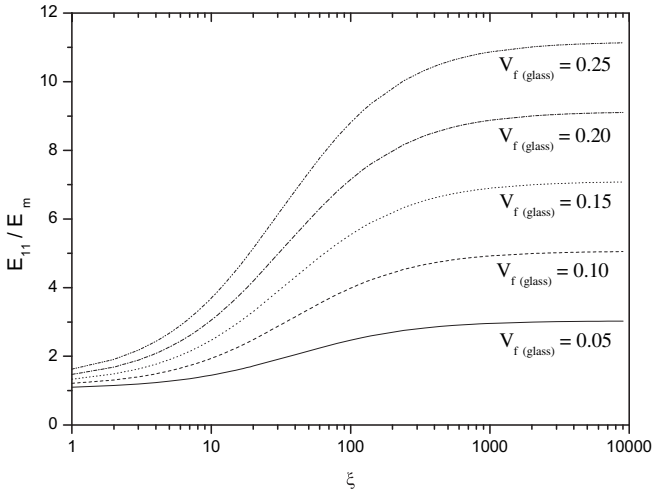

Fig. 2. The effect of ξ and $V_{f(glass)}$ on the relative modulus of GF/PA along the longitudinal axis predicted by the Halpin-Tsai equations.

such a high modulus as clay platelets. For example, clay at 5% volume at $\xi = 100$ could contribute to 3.5 in the relative modulus, whereas, glass fibres only give a doubling in the relative modulus at the same volume fraction and shape factor. Thus, increasing the filler modulus improves the reinforcement. In realistic short glass fibre composites, the aspect ratio of glass fibres is normally 20–50 and so has less effect on the modulus than clay.

In order to compare the effect of the two reinforcements, ξ and V_f of the relative modulus are evaluated in Fig. 3. Increasing ξ and V_f in both fillers leads to an increase in the modulus. If clay is not exfoliated (at low $\xi_{clay} = 10$), the effect of clay is similar to that of glass fibre (at $\xi_{glass} = 10$); this indicates that although clay has nearly twice the modulus of glass fibre, it can provide the same reinforcement effect as glass fibre at low ξ. However, if clay is fully exfoliated (at high $\xi_{clay} = 200$), PA/Clay have a significantly higher modulus compared to GF/PA. From this figure, we conclude that exfoliation is crucial to achieve high modulus. From TEM observations, the aspect ratio of clay was found to be between 50 and 250, which is within the range that the Halpin-Tsai model predicts [17]. The aspect ratio of glass fibre is 20–30 in GF/PA. Compared to that of

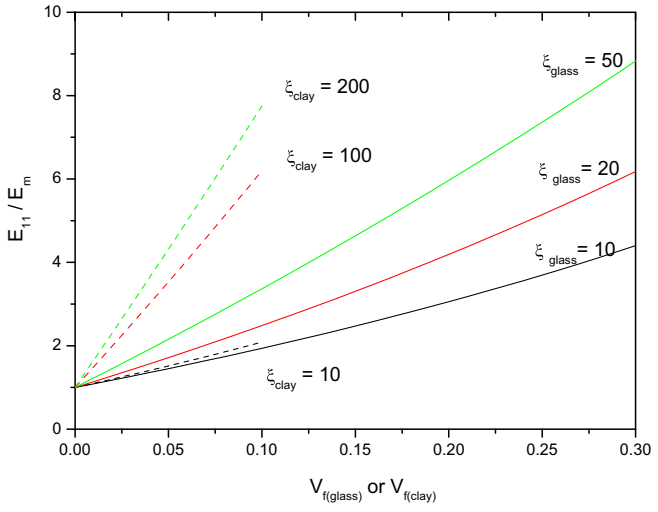

Fig. 3. A comparison of clay and glass fibre in ξ and V_f on the relative modulus along longitudinal axis predicted by the Halpin-Tsai equations.

GF/PA, the modulus of PA/Clay increases significantly at the same value of ξ and V_f. Thus, the higher modulus caused by clay is a combination of the higher $E_{f(clay)}$ and ξ_{clay}, which leads to dramatic differences in the modulus for GF/PA and PA/Clay.

A crucial question is the effect of a combination of clay platelets and glass fibres on the modulus. To simplify the question, we assume that it is not any interaction between clay and glass fibres. PA/Clay as a matrix is reinforced by glass fibre. The Halpin-Tsai model is applied to predict the modulus of GF/PA/Clay.

To calculate the modulus of PA/Clay; the equation can be written as follows:

$$\frac{E_{c(PA/Clay)}}{E_m} = \frac{\left(1+\xi_{(clay)}\eta_{(clay)}V_{f(clay)}\right)}{1-\eta_{(clay)}V_{f(clay)}} \tag{2}$$

$$\text{in which } \eta_{(clay)} = \frac{E_{f(clay)}/E_m - 1}{E_{f(clay)}/E_m + \xi_{(clay)}}$$

To calculate the modulus of GF/PA/Clay, the equation can be written as Equations (3) and (4). In the second model, the result of the modulus of PA/Clay from Equation (2) is used as the modulus of the matrix of the GF/PA/Clay composite. The relative modulus of GF/PA/Clay in longitudinal and transversal directions can be calculated from Equations (3) and (4), and then Krenchel's approach is applied to predict the relative modulus according to Equation (5). The relative modulus of GF/PA can be calculated from Equation (6) directly. In order to calculate the modulus of GF/PA/Clay, ξ_{clay} and $V_{f(clay)}$ of PA/Clay must be calculated first.

$$\frac{E_{11(GF/PA/Clay)}}{E_m} = \frac{\left(1+\xi_{(glass)}\eta_{(glass)}V_{f(glass)}\right)}{1-\eta_{(glass)}V_{f(glass)}} * \frac{E_{c(PA/clay)}}{E_m} \tag{3}$$

$$\frac{E_{\perp(GF/PA/Clay)}}{E_m} = \frac{\left(1+2\eta_{(glass)}V_{f(glass)}\right)}{1-\eta_{(glass)}V_{f(glass)}} * \frac{E_{c(PA/clay)}}{E_m} \tag{4}$$

in which

$$\eta_{(glass)} = \frac{E_{f(glass)}/E_{c(clay)} - 1}{E_{f(glass)}/E_{c(clay)} + \xi_{(glass)}}$$

$$\frac{E_{c(GF/PA/Clay)}}{E_m} = \eta_0\frac{E_{11(GF/PA/Clay)}}{E_m} + (1-\eta_0)\frac{E_{\perp(GF/PA/Clay)}}{E_m} \tag{5}$$

$$\frac{E_{c(GF/PA)}}{E_m} = \eta_0\frac{E_{11(GF/PA)}}{E_m} + (1-\eta_0)\frac{E_{\perp(GF/PA)}}{E_m} \tag{6}$$

E_m, $E_{c(clay)}$, ξ_{glass} and η_0 were measured and calculated from experimental data. The orientation of fillers has a dramatic effect on the modulus of composites. From a practical point of view, all fillers filled composites contain various degrees of filler misalignment. This misalignment can result in the reduction of composite modulus. One of the most useful methods for evaluating the relative efficiency of fibre reinforcement in each orientation is Krenchel's approach. According to experimental data, the orientation distributions for the two samples are slightly different, so η_0 for GF/PA/Clay and GF/PA are calculated for each samples [17].

4. Experimental results and prediction for modulus of composites

Besides the predictions of the composite modulus, the Halpin-Tsai model can also be used to calculate ξ_{clay} when the modulus of the PA/Clay, PA and clay are known. It should be mentioned that the

orientation of clay platelets cannot be measured by current instruments, so an orientation efficiency (η_0) cannot be precisely predicted. Therefore, most of the modulus of filler composites are predicted by the Halpin-Tsai model and do not consider η_0. Thus, the Halpin-Tsai model can only predict ξ_{clay}, rather than the aspect ratio, because the clay platelets have different shapes, sizes and thicknesses. ξ_{clay} were derived from the Halpin-Tsai model for nanocomposites. This represents the best fit with the measured modulus and can be considered a useful parameter to compare other nanocomposites, as well as providing a reasonable estimate of the average aspect ratio. The Halpin-Tsai model predicts E_c/E_m and the value of ξ_{clay} for the best fit with the experimental results. The experimental results in Fig. 4 show a rapid increase in modulus with $V_{f(clay)}$. The modulus increased by a factor of 1.7 as $V_{f(clay)}$ increased from zero to 1.5%. The value of ξ_{clay} was estimated by selecting an appropriate value for the best fit to the experimental data. Comparing the predictions and experimental data, the fitted value of ξ_{clay} changes from 80 to 60 with $V_{f(clay)}$. From this prediction, the reason for the high modulus enhancement of PA/Clay may be attributed to the larger ξ_{clay}. It is plausible that the decrease of ξ_{clay} results from the tendency of agglomeration of clay platelets with increasing $V_{f(clay)}$ or length reduction due to the collision of clay platelets. It is worth to note that the strong interaction between clay and PA is another important contribution for the modulus.

In order to study the effect of $V_{f(glass)}$ on the relative modulus of GF/PA/Clay, $V_{f(clay)}$ must be fixed. 5% of clay in weight ($V_{f(clay)} = 1.5\%$) was chosen as a PA/Clay matrix. The composite produced when glass fibres are combined with this matrix is denoted GF/PA/Clay5. Fig. 5 shows the results of tensile modulus and predictions of GF/PA/Clay5 compared to GF/PA. Tensile tests show an increase in modulus with $V_{f(glass)}$ for GF/PA and GF/PA/Clay5. The two solid lines are the predictions of the relative modulus, taking fibre orientation into account. From the analysis of experimental data and predictions, the relative modulus of GF/PA/Clay5 is higher than that of GF/PA at the same $V_{f(glass)}$. The predictions fit well with the experimental data for GF/PA, but over-predict the modulus for GF/PA/Clay5.

To study the effect of $V_{f(clay)}$ on the relative modulus of GF/PA/Clay, $V_{f(glass)}$ is fixed. 20% of glass fibre by weight (around 10% of glass fibre by volume) was chosen as reinforcement. The glass fibre filled PA/Clay matrix is denoted as GF20/PA/Clay. Fig. 6 shows the

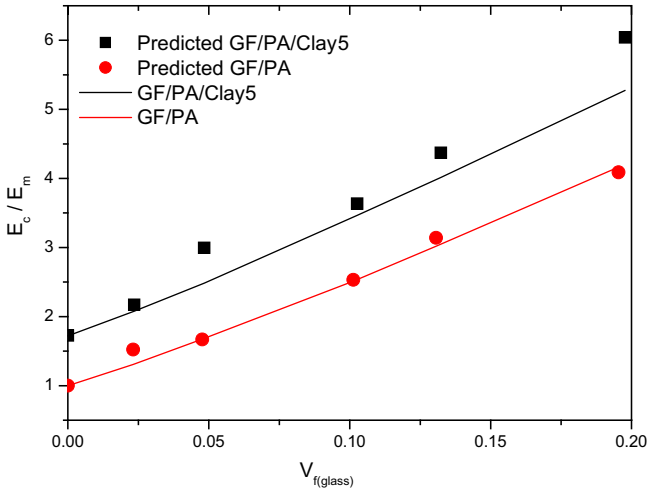

Fig. 5. A comparison of predictions and experimental data for the effect of $V_{f(glass)}$ on the relative modulus of GF/PA/Clay5.

results of tensile modulus and predictions of GF20/PA/Clay compared to PA/Clay. The results show the addition of clay in the matrix significantly increases the tensile modulus for both PA/Clay and GF20/PA/Clay. From the analysis of experimental data and predictions, the relative modulus of GF20/PA/Clay is higher than that of PA/Clay at the same $V_{f(clay)}$. The dash line is the predicted modulus of GF20/PA/Clay according to Equation (5). The solid line is the predicted modulus of PA/Clay according to Equation (2). The slopes of the two curves are roughly parallel. According to Figs. 5 and 6, applying the Halpin-Tsai model to the data measured from tensile tests suggests that the combination of glass fibre and clay in polymer matrix has a higher reinforcing effect than each of individual fillers. The experimental results showed a deviation between the prediction and experimental data for GF/PA/Clay, so a correction factor (η_1) is applied and the equation (5) can be written as Equation (7). η_1 is calculated to satisfy the experimental results.

$$\frac{E_{c(GF/PA/Clay)}}{E_m} = \eta_1\left(\eta_0\frac{E_{11(GF/PA/Clay)}}{E_m} + (1-\eta_0)\frac{E_{\perp(GF/PA/Clay)}}{E_m}\right) \tag{7}$$

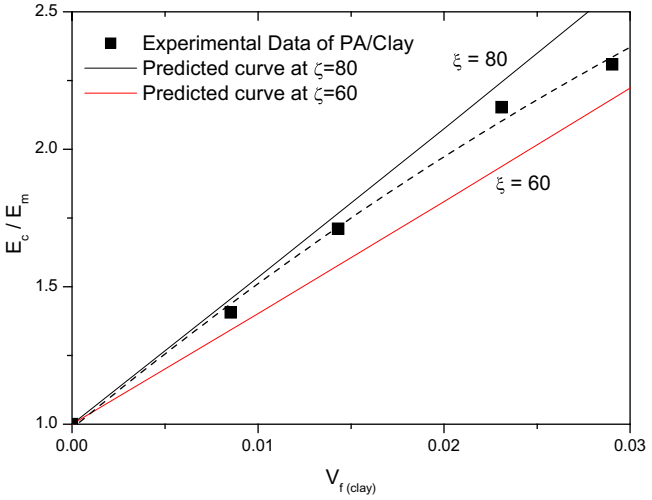

Fig. 4. A comparison of predictions and experimental data for the effect of $V_{f(clay)}$ on the relative modulus of PA/Clay.

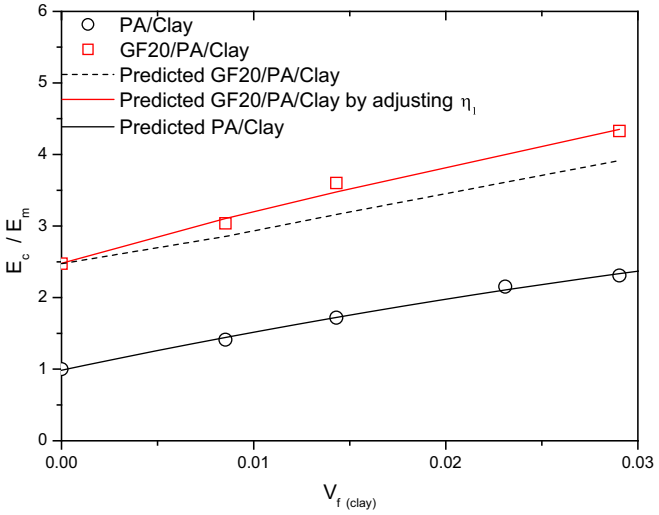

Fig. 6. A comparison of predictions and experimental data for the effect of $V_{f(clay)}$ on the relative modulus of GF20/PA/Clay.

From Fig. 6, the experimental data of the relative modulus for glass filled PA/Clay is higher than the predictions. The predicted modulus of the GF/PA/Clay in the longitudinal and transversal directions is adjusted by a correction factor (η_1) to fit the experimental data, so that the modulus of GF/PA/Clay can be well predicted by Halpin-Tsai model. The effect of $V_{f(clay)}$ on the predicted η_1 for GF20/PA/Clay is shown in Fig. 7. The value of η_1 is estimated by selecting an appropriate value for the best fit to the experimental data. With increasing clay loadings, η_1 increases dramatically. The synergistic effect can be estimated by the value of η_1. When $V_{f(clay)}$ only increased to 3%, around 12% of the synergistic effect on the modulus can be observed. It can be concluded that adding clay and glass fibre causes a synergy between the reinforcements at the two different scales. The synergy greatly affects the final mechanical properties of the samples.

This suggests that two fillers in different scales (glass fibre at the micro-scale and clay at the nanoscale) in polymer matrix have a synergistic effect and a higher reinforced ability than each of individual filler. This could be due to four factors: firstly, the inclusion of clay enhances the orientation of fibres along the test specimen [17]. It has been demonstrated that the viscosity of PA is altered significantly by the inclusion of clay. However, the fibre orientation results are taken into account on the alignment effect on fibres in each case, and it is therefore unlikely that there is any enhanced orientation effect. Secondly, we must consider if the inclusion of clay increases the length of the glass fibres. Experimental evidence suggests that the inclusion of clay decreases the length distribution of fibres in the injection-moulded sample. As the fibres pass through the extruder and the injection moulding machine, there is a significant degradation in fibre length, especially in the injection process. Thirdly, the reduction in viscosity achieved by adding clay assists mould filling and reduces voids. Whilst this is true, the PA/GF samples contain less than 1% voids so the effect on mechanical properties is slight. Fourthly, we suggest that there is some interaction between the nano and micro-scale reinforcement. This is the most interesting scenario, and in our opinion, the most likely explanation. Thus, a correction factors (η_1) is introduced to explain the apparent increase in the modulus of GF/PA/Clay5, when applying the Halpin-Tsai approach to the data measured from tensile tests.

Weight saving is a very important factor for evaluating the applications of materials. Fig. 8 demonstrates the specific modulus increases with density (ρ) caused by the addition of clay and glass fibres. PA/Clay provides a higher specific modulus than GF/PA and GF/PA/Clay at ρ below 1.17 g/cm^3, but GF/PA/Clay has larger modulus

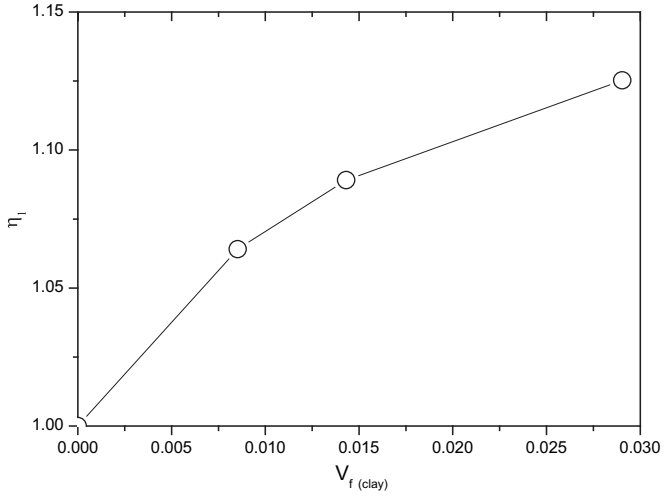

Fig. 7. The effect of $V_{f(clay)}$ on the predicted correction factor (η_1) of GF20/PA/Clay.

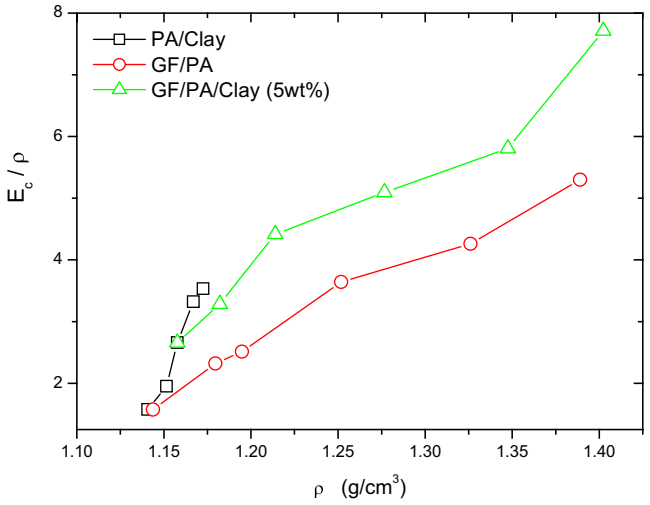

Fig. 8. The effect of ρ on the specific modulus.

contribution, compared to GF/PA at ρ above 1.17 g/cm^3. We believe that the glass fibre filled nanocomposites are of commercial interests, as it can increase the overall mechanical properties.

5. Conclusions

The Halpin-Tsai model has been successfully applied to model the improvement in tensile modulus of nanocomposites. The model can be used when a polymer is reinforced with nano particles of clay and with micro-scale glass fibres. We have shown that there is synergy in combining these disparate reinforcements; the weight saving is achieved by including clay in glass fibre composites, which enhances and allows the higher modulus of materials to be manufactured. In addition, there appears to be some beneficial synergy between the two scales of reinforcement, which merits further investigation.

The analysis makes the assumption that the reinforcement phases are fully aligned and of uniform shape/geometries. Although these assumptions are far from true for practical composites, the modelling approach works well. However, the non-uniformity should be considered and is an area for future research.

References

[1] Hull D, Clyne TW. An introduction to composites materials. UK: Cambridge University Press; 1981.
[2] Krishnamoorti R, Ren J, Silva AS. Journal of Chemical Physics 2001;114:4968–78.
[3] Gonzáleza I, Eguiazábala JI, Nazábal J. Polymer 2005;46:2978–85.
[4] LeBaron PC, Wang Z, Pinnavaia TJ. Applied Clay Science 1999;15:11–29.
[5] Yasue K, Katahira S, Yoshikawa M, Fujimoto K. In situ polymerisation route to nylon 6-clay nanocomposites. In: Pinnavaia TJ, Beall GW, editors. Polymer-clay nanocomposites. John Wiley & Sons Ltd; 2000. p. 112–26.
[6] Liu XH, Wu Q. Polymer 2002;43:1933–6.
[7] Hu X, Zhao XY. Polymer 2004;45:3819–25.
[8] Wan T, Clifford MJ, Gao F, Bailey AS, Gregory DH. Polymer 2005;46:6429–36.
[9] Loo LS, Gleason KK. Macromolecules 2003;36:2587–90.
[10] Mallik PK. Particulate and short fibre reinforced polymer composites, in comprehensive composites materials; 2000. p. 291–331.
[11] Halpin JC, Kardos JL. Polymer Engineering and Science 1976;16:344–52.
[12] Nielsen EL, Landel RF. Mechanical properties of polymers and composites. New York: Marcel Dekker, Inc; 1994.
[13] Fornes TD. Polymer 2003;44:4993–5013.
[14] Halpin JC, Finlayson KM, Ashton JE. Primer on composites materials. CRC Press; 1992.
[15] Vlasveld DPN. Fibre reinforced polymer nanocomposites. PhD Thesis. Delft University; 2005.
[16] Sheng N, Boyce MC, Parks DM, Rutledge GC, Abes JI, Cohen RE. Polymer 2004;45:487–506.
[17] Wan T. Characterisation of PA/clay nanocomposites and glass fibre filled PA/clay nanocomposites. PhD Thesis. UK: The University of Nottingham; 2006.